



Charged impurity scattering in bilayer graphene

Shudong Xiao,^{1,2} Jian-Hao Chen,^{1,2} Shaffique Adam,^{1,3} Ellen D. Williams,^{1,2} and Michael S. Fuhrer^{1,2,*}

¹Center for Nanophysics and Advanced Materials, University of Maryland, College Park, Maryland 20742, USA

²Materials Research Science and Engineering Center, University of Maryland, College Park, Maryland 20742, USA

³Condensed Matter Theory Center, Department of Physics, University of Maryland, College Park, Maryland 20742, USA

(Received 8 August 2009; revised manuscript received 3 May 2010; published 16 July 2010)

We have examined the impact of charged impurity scattering on charge carrier transport in bilayer graphene (BLG) by deposition of potassium in ultrahigh vacuum at low temperature. Charged impurity scattering gives a conductivity which is supralinear in carrier density with a magnitude similar to single-layer graphene for the measured range of carrier densities of $2-4 \times 10^{12} \text{ cm}^{-2}$. Upon addition of charged impurities of concentration n_{imp} , the minimum conductivity σ_{min} decreases proportional to $n_{\text{imp}}^{-1/2}$ while the electron and hole puddle carrier density increases proportional to $n_{\text{imp}}^{1/2}$. These results for the intentional deposition of potassium on BLG are consistent with theoretical predictions for charged impurity scattering assuming a gapless hyperbolic dispersion relation. However, our results also suggest that charged impurity scattering alone cannot explain the observed transport properties of pristine BLG on SiO_2 before potassium doping.

DOI: [10.1103/PhysRevB.82.041406](https://doi.org/10.1103/PhysRevB.82.041406)

PACS number(s): 72.10.Fk

Bilayer graphene (BLG) (Refs. 1 and 2) is a unique electronic material distinct from single-layer graphene (SLG):³ while SLG has a massless, gapless electronic dispersion $E(k) = \pm \hbar v_F |k|$, BLG has a low-energy dispersion which is approximated^{2,4} by massive valence and conduction bands with zero gap: $E(k) = \pm \hbar^2 k^2 / 2m^*$, where the effective mass is $m^* = \gamma_1 / 2v_F^2$, with $\gamma_1 \approx 0.39 \text{ eV}$ the interlayer hopping matrix element, $v_F \approx 1.1 \times 10^6 \text{ m/s}$ the Fermi velocity in single layer graphene, and \hbar Planck's constant. BLG has attracted interest because of a tunable bandgap,⁵⁻⁸ and unusual quantum-Hall physics with an eightfold degenerate zero-energy Landau level.¹ However, little is known about disorder and charge-carrier scattering in BLG. Similar to SLG, linear $\sigma(n)$ is observed experimentally⁹ with mobilities limited to $< 10^4 \text{ cm}^2/\text{Vs}$. However, unlike SLG, linear $\sigma(n)$ is expected for both charged impurities and short-range scatterers within the complete screening approximation¹⁰⁻¹² hence the dominant disorder scattering mechanism in BLG remains an open question.

SLG provides a starting point for understanding the effects of disorder in BLG. In SLG on SiO_2 substrates¹³ impurity scattering is dominated by charged impurities with a typical density n_{imp} of a few 10^{11} cm^{-2} , which give rise to a linear conductivity as a function of charge carrier density, i.e., $\sigma(n) = ne\mu$ (Refs. 14 and 15) with constant mobility μ , with additional contributions from weak short-range scatterers with $\sigma(n) \sim \text{constant}$.¹⁶ At low n , the random potential from charged impurities produces electron and hole puddles with a characteristic carrier density n^* , giving rise to a minimum conductivity $\sigma_{\text{min}} = n^* e \mu \approx (4-10)e^2/h$. To leading order, $n^* \propto n_{\text{imp}}$ and $\mu \propto n_{\text{imp}}^{-1}$ so σ_{min} varies only weakly with n_{imp} .^{14,17} Charged impurities have been predicted to lead to stronger scattering in BLG compared to SLG,¹⁰ consistent with the generally lower mobilities observed for BLG compared to SLG. However, as we discuss below, this prediction was based on two severe approximations for the bilayer case (complete screening and zero impurity-graphene distance) and a more complete treatment indicates that BLG and SLG should have similar mobility for a similar density of charged

impurity scatterers. In contrast to SLG, the random charged impurity potential in BLG is well-screened, and $n^* = (n_{\text{imp}}/\xi^2)^{1/2}$, i.e., n^* is simply the fluctuation in the impurity number within an area given by the square of the puddle correlation length ξ . This leads to a strong prediction for the variation of the minimum conductivity on the density of trapped charges $\sigma_{\text{min}} \propto n_{\text{imp}}^{-1/2}$ which can be tested experimentally.

Here we experimentally measure the scattering rate for charged impurities on BLG by depositing potassium on BLG in ultrahigh vacuum (UHV) at low temperature. Charged impurity scattering gives a carrier-density-dependent conductivity $\sigma(n)$ which is supralinear in n with similar magnitude to single layer graphene for the measured range of carrier densities of $2-4 \times 10^{12} \text{ cm}^{-2}$. The conductivity is in good agreement with that calculated within the Thomas-Fermi (TF) screening approximation¹⁰ once the finite screening length and impurity-graphene distance are taken into account. The dependence of the minimum conductivity and the residual carrier density on charged impurity density are well-described by $\sigma_{\text{min}} \propto n_{\text{imp}}^{-1/2}$ and $n^* = (n_{\text{imp}}/\xi^2)^{1/2}$ in agreement with theoretical expectations, though the puddle correlation length ξ is significantly larger than predicted theoretically. The theoretical model we consider here ignores the opening of a band gap, an approximation that is valid only when the disorder-induced potential fluctuation is much larger than the band gap. The absence of any transport gap in our experiments suggests that the disorder potential is surprisingly large and more work is needed to understand why the gapless model describes our data. Most important, however, the experimentally measured magnitude and carrier-density dependence for charged impurity scattering on BLG indicates that unlike SLG, charged impurities alone cannot explain the observed transport behavior of pristine BLG samples on SiO_2 , i.e., before the intentional addition of charged impurities. We infer the presence of an additional source of disorder in the undoped BLG that gives rise to $\sigma(n) \sim n$.

BLG is mechanically exfoliated from Kish graphite onto 300 nm SiO_2 on Si substrates. See supplementary material

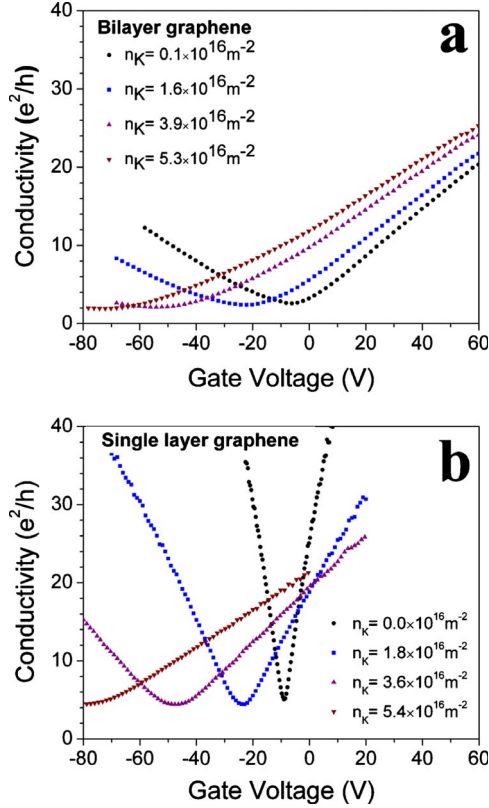


FIG. 1. (Color online) The conductivity (σ) versus gate voltage (V_g) curves for different potassium concentrations for BLG (a) and SLG (b). For BLG, $\sigma(V_g)$ is measured at a temperature of 10 K in UHV. Data in (b) are from Ref. 14.

for a photomicrograph of the device.¹⁸ Au/Cr electrodes are defined by electron-beam lithography and the doped Si acts as a back gate. Bernal stacking of the BLG was verified by micro-Raman spectroscopy (see supplementary material for Raman spectrum¹⁸). The Raman G' band showed four Lorentzian components with relative peak positions and magnitudes similar to those in Ref. 19, indicative of Bernal stacking.¹⁸ After annealing in H_2/Ar at 400 °C,²⁰ the device was mounted on a cold finger in UHV chamber and an overnight bakeout was performed in vacuum. In UHV, the charged-impurity density n_{imp} was varied systematically by deposition of potassium atoms from a controlled source at a sample temperature $T=10$ K. Conductivity as a function of gate voltage $\sigma(V_g)$ was measured *in situ* at different K concentrations; the carrier concentration is given by $n = (c_g/e)(V_g - V_{g,min}) = [7.2 \times 10^{10} \text{ cm}^{-2} \text{ V}^{-1}](V_g - V_{g,min})$ with $c_g = 1.15 \times 10^{-8} \text{ F/cm}^2$ the gate capacitance per unit area and $V_{g,min}$ the gate voltage of minimum conductivity.

Figure 1(a) shows $\sigma(V_g)$ measured at different K doses for BLG and, for comparison, Fig. 1(b) shows similar data for SLG taken from Ref. 14. Before K doping, the annealed BLG sample has a lower mobility (1200 cm^2/Vs) than pristine SLG prepared similarly (13 000 cm^2/Vs). This is typical for our H_2/Ar annealed BLG samples, which show mobility 2–5 times lower than unannealed BLG, and ~ 10 times lower than SLG devices on the same SiO_2 substrates (annealing SLG does not appreciably change the mobility). K dop-

ing shifts the transport curve to the negative gate voltage side, lowers the mobility, decreases σ_{min} , broadens the minimum conductivity plateau and makes the $\sigma(V_g)$ curve nonlinear.

For uncorrelated impurities, the mobility is inversely proportional to the impurity density $\mu = \frac{C}{n_{imp}}$. The nonlinearity of $\sigma(V_g)$ indicates that mobility, and thus C , is a function of carrier density, unlike SLG where C is a constant. To quantify our results we introduce an initial impurity density $n_{imp,0}$ so that the total impurity density is $n_{imp} = n_{imp,0} + n_K$, where n_K is the potassium concentration. While the charged impurities corresponding to $n_{imp,0}$ could, in principle, have opposite charge or be at a different distance from the bilayer graphene sheet than n_K , to avoid introducing too many parameters, and consistent with results from residual impurities on single-layer graphene,¹⁶ we assume $\frac{1}{\mu(n)} = \frac{n_{imp,0}}{C(n)} + \frac{n_K}{C(n)}$. We assume that n_K is given by the shift of $V_{g,min}$, i.e., $n_K = (c_g/e)\Delta V_{g,min}$ which is exact within the parabolic approximation for the BLG Hamiltonian;¹⁰ below we show that for the range of densities we consider, this approximation remains very good for the hyperbolic Hamiltonian.

Figure 2(a) shows the inverse electron mobility $1/\mu$ as a function of n_K at $V_g=30$ V and 60 V for BLG. $1/\mu$ vs n_K is linear as expected and we determine $C(n)$ as the inverse of the slope of $1/\mu$ vs n_K , yielding $C(60 \text{ V}) = 5.1 \times 10^{15} \text{ V}^{-1} \text{ s}^{-1}$ and $C(30 \text{ V}) = 4.2 \times 10^{15} \text{ V}^{-1} \text{ s}^{-1}$. For $V_g < 30$ V the measurement is influenced by the minimum conductivity region, and $1/\mu$ vs n_K is not linear, so C could not be extracted. For BLG, $n_{imp,0}$ varies systematically from $3.4 \times 10^{16} \text{ m}^{-2}$ at $V_g=30$ V to $4.3 \times 10^{16} \text{ m}^{-2}$ at $V_g=60$ V. We find that the initial impurity density $n_{imp,0}$ for BLG is one order of magnitude higher than for SLG (see discussion below), the data for which are shown for comparison.

Figure 2(b) shows the complete measured dependence of $C(V_g)$ for BLG (solid squares). Data from a second sample is also shown (solid circles) with similar results. For comparison, the SLG value, $C=5 \times 10^{15} \text{ V}^{-1} \text{ s}^{-1}$ (Ref. 14) is shown in blue. The similarity to the values for BLG indicates that the scattering cross section for charged impurities in BLG is very similar to SLG. The black line shows the previously calculated result^{10,21} for $C(V_g)$ within the complete screening approximation with $d=0$. The red/gray line with open circle and purple/gray line with upward-pointing triangle show $C(V_g)$ calculated within the TF approximation without making the complete-screening approximation¹⁰ for impurity-graphene distances $d=0$ (red) and $d=0.43$ nm (purple; the expected potassium-graphene distance of 0.26 nm (Ref. 22) plus one-half the interlayer separation of 0.34 nm). The experimental data are close to the TF calculation with somewhat smaller magnitude and less carrier density dependence.^{18,23–25}

Figure 3 shows σ_{min} as a function of n_K . The minimum conductivity decreases with increasing charged impurity concentration. The residual carrier density $n^* = \sigma_{min}/e\mu = \sigma_{min}(n_{imp,0} + n_K)/eC$. Since we do not know the mobility at $V_g=0$, we use $C(30 \text{ V}) = 4.2 \times 10^{15} \text{ V}^{-1} \text{ s}^{-1}$ and $n_{imp,0}(30 \text{ V}) = 3.4 \times 10^{16} \text{ m}^{-2}$ to estimate $\mu = C/(n_{imp,0} + n_K)$. Figure 3 shows n^* as a function of n_K . n^* increases with charged impurity doping, as expected. The solid lines in Fig.

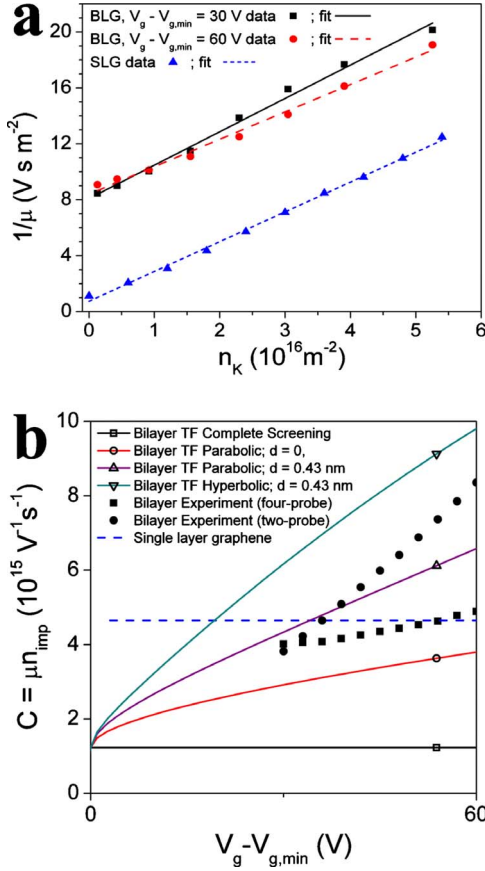


FIG. 2. (Color online) (a) Inverse of electron mobility $1/\mu$ versus potassium concentration n_K . Line are linear fits to all data points used to extract the slope $1/C$. μ is the maximum field-effect mobility for SLG (data from Ref. 14) and is shown at two different carrier densities for BLG. (b) The inverse slope C from (a) versus effective gate voltage (solid black squares). Also shown is a second set of data from a different sample measured in a two-probe configuration (solid black circles). Solid lines show the theoretical predictions for C within the Thomas-Fermi approximation for a parabolic dispersion relation assuming complete screening (black line) and finite TF screening wave vector with impurity graphene distance $d=0$ (red/gray with an open circle) and $d=0.43 \text{ nm}$ (purple/dark gray with an open upward-pointing triangle). The green/gray with an open downward-pointing triangle line shows the theoretical results for a hyperbolic dispersion relation with finite TF screening wavevector and $d=0.43 \text{ nm}$. The SLG value is also shown (blue dashed line) for comparison (Ref. 14).

3 show fits to the theoretically predicted behavior $n^* = [(n_{\text{imp},0} + n_K)/\xi^2]^{1/2}$ and $\sigma_{\min} = Ce[(n_{\text{imp},0} + n_K)\xi^2]^{-1/2}$. The only free parameter ξ is found to be 32 nm. This is significantly larger than the correlation length $\xi=9 \text{ nm}$ calculated within the self-consistent model using TF screening. We likely overestimated C by as much as a factor of 3 in using $C(30 \text{ V})$ [see Fig. 2(b)] and therefore ξ may be as much as 40% smaller ($\sim 18 \text{ nm}$) but still twice the calculated value. A similar discrepancy (self-consistent theory overestimating n^*) is found in SLG.¹⁴

The theoretical results discussed above rely on the parabolic approximation for the dispersion relation for BLG,² only valid for carrier densities much lower than n_0

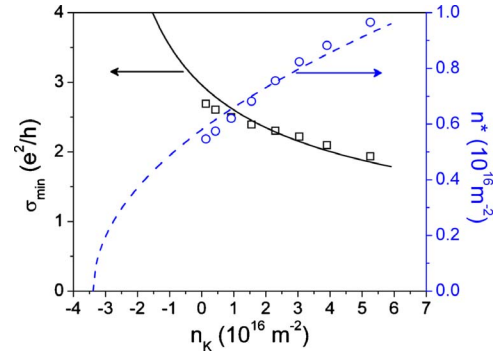


FIG. 3. (Color online) Minimum conductivity σ_{\min} and residual carrier density n^* of bilayer graphene as a function of potassium concentration n_K . The blue (dashed) and black (solid) lines show fits to $n^* = [(n_{\text{imp},0} + n_K)/\xi^2]^{1/2}$ and $\sigma_{\min} = Ce[(n_{\text{imp},0} + n_K)\xi^2]^{-1/2}$ with C and $n_{\text{imp},0}$ determined from the fit to $1/\mu$ vs n_K at $V_g = 30 \text{ V}$ in Fig. 2(a), and $\xi = 32 \text{ nm}$.

$= (v_F m^*/\hbar)^2 / \pi \sim 2 \times 10^{12} \text{ cm}^{-2}$. The experimental results presented here cross over from this low density limit to much higher densities where the parabolic approximation for the Hamiltonian breaks down. We briefly examine the robustness of the theoretical results for BLG transport at low density¹⁰ to the situation when the carrier density (or equivalently, the impurity density) is much larger than n_0 . Our main finding is that the results for higher density are qualitatively very similar to those found using the parabolic approximation. The crossover Hamiltonian reads² $H = \sigma_x \otimes [v_F(\sigma_x, \sigma_y) \cdot \hbar \vec{k}] + [(I_2 - \sigma_z)/2] \otimes \gamma_1 \sigma_x$, where I_2 is the identity matrix and $\sigma_{x,y,z}$ are the Pauli matrices. The dispersion relation is hyperbolic, with $E_b = \hbar^2 k^2 / (2m^*)$ and $E_s = \hbar v_F |k|$ as the low density and high density asymptotes, where $v_F = 1.1 \times 10^6 \text{ m/s}$ is the SLG Fermi velocity and $m^* = \gamma_1 / (2v_F^2) \approx 0.033m_e$ is the low density effective mass for BLG. Analogous to the treatment in Ref. 26 for SLG, for the crossover Hamiltonian the scattering time reads

$$\frac{\hbar}{\tau[\varepsilon(k)]} = 2\pi \sum_{k'} n_{\text{imp}} \left| \frac{v(q,d)}{\varepsilon(q)} \right|^2 F(\theta)(1 - \cos \theta) \delta[\varepsilon(k) - \varepsilon(k')], \quad (1)$$

where the wave function overlap $F(\theta) = (1/4)[1 - \eta + (1 + \eta)\cos \theta]^2$, and $\eta = (1 + n/n_0)^{-1/2}$ parameterizes the crossover. Within TF, the dielectric function $\varepsilon(q, n) = 1 + v(q)v(n)$, and density of states $\nu(n) = (2m^*/\pi\hbar)\sqrt{1 + n/n_0}$. The mobility calculated using Eq. (1) is shown in Fig. 2(b) (green/gray line with downward-pointing open triangle). As seen in the figure, while the modified Hamiltonian gives a slightly larger mobility, it is not significantly different from the low density parabolic dispersion approximation.

We can also examine the transport properties at low density, close to the Dirac point. Applying the self-consistent transport theory¹⁷ to the parabolic approximation for bilayer graphene¹⁰ gives $\bar{n} \equiv (\frac{C\xi}{e})V_{g,\min} = n_{\text{imp}}$ and $n^* = [n_{\text{imp}}/\xi^2]^{1/2}$. Using the crossover Hamiltonian we find $n^* \approx n_{\text{imp}} C_0 [\alpha\sqrt{n^*/n_0}] + \sqrt{4n_{\text{imp}}n_0 C_0 [\alpha\sqrt{n^*/n_0}]}$, where $\alpha = 4d\sqrt{2\pi n_0}$ and $C_0[x] = \partial_x [xe^x \int_x^\infty t^{-1} e^{-t} dt]$. The numerical solu-

tion for the electron and hole puddle density using the crossover Hamiltonian is remarkably close to the parabolic result $n^* = [n_{\text{imp}}/\xi^2]^{1/2}$ with only about a 5% decrease in the value of ξ . The correction to \bar{n} is more significant

$$\frac{\bar{n}}{n_{\text{imp}}} \approx \left[\frac{n_{\text{imp}}/n_0 + 4\sqrt{1 + \sqrt{\beta n_{\text{imp}}}}}{4(1 + \sqrt{\beta n_{\text{imp}}})} \right], \quad (2)$$

where $\beta = 1/\xi^2 n_0^2 \approx 6.4 \times 10^{-13} \text{ cm}^2$ and the right-hand side of Eq. (2) changes from unity at low impurity density to about 0.8 for the highest impurity densities we consider. This indicates that we may have underestimated the impurity concentration from $n_{\text{imp}} = \bar{n}$ by up to $\sim 20\%$, which would indicate that $C(n)$ may be higher than shown in Fig. 2(b) by up to $\sim 20\%$.

Overall, the magnitude and carrier-density dependence of C and the impurity density dependence of n^* and σ_{min} are in good qualitative agreement with the theory of charged impurity scattering in BLG. However, C is somewhat smaller, and ξ somewhat larger, than expected theoretically, which both indicate that screening is not as effective as predicted. A possible explanation is the opening of a gap at the Dirac point in biased bilayer graphene,^{5–8} which we have not treated theoretically. The reduced screening in gapped BLG has also been put forth to explain the dependence of flicker noise on gate voltage in BLG.²⁷ One can expect that the signatures in transport experiments of the electric field-induced band gap to be negligible when the disorder potential fluctuation is much larger than the band gap.²⁸ From the optical measurements of Ref. 7 we can estimate that the maximum band gap we would induce is about 100 meV, while for $n_{\text{imp}} = 5.3 \times 10^{12} \text{ cm}^{-2}$, we can estimate the unscreened disorder potential to be about 200 meV. Surpris-

ingly, even though the band gap is similar in magnitude to the disorder potential, the theory which neglects band gap describes the data reasonably well; more work is needed to understand this in detail. We expect the opening of a band gap in BLG to have an even smaller effect on transport in the high-density regime [data in Fig. 2(b)], where the change in density of states at the Fermi energy in BLG induced by gap opening is estimated to be a few percent.

Lastly, we discuss the nature of scattering in BLG on SiO₂. Our experimental finding that the magnitude of charged-impurity scattering in BLG is similar to SLG is surprising given that pristine BLG typically shows lower mobility (~ 10 times for our H₂/Ar annealed samples) than SLG on nominally identical SiO₂ substrates. We note that the H₂/Ar annealing process itself significantly lowers the mobility of BLG without affecting SLG, which is not understood. The variation in C with V_g is also inconsistent with the linear $\sigma(V_g)$ observed in BLG.⁹ Together, these observations indicate that another source of disorder may dominate BLG on SiO₂. This may be consistent with observations of reduced noise (presumably due to fluctuations of charged impurities) in BLG compared to SLG.²⁹ Further work is needed to clarify that source of scattering in undoped BLG on SiO₂. Measurement of the variation in the mobility with dielectric constant¹⁶ could potentially discriminate between charged-impurity and short-range disorder.

This work has been supported by the NSF-UMD-MRSEC under Grant No. DMR 05-20471 (E.D.W.) and the U.S. ONR MURI under Grant No. N000140911064. The MRSEC shared equipment facilities were used in this work. Infrastructure support has also been provided by the UMD Nano-Center and CNAM. We thank S. Das Sarma for useful discussions regarding this manuscript.

*mfuhrer@umd.edu

- ¹K. S. Novoselov *et al.*, *Nat. Phys.* **2**, 177 (2006).
- ²E. McCann and V. I. Fal'ko, *Phys. Rev. Lett.* **96**, 086805 (2006).
- ³K. S. Novoselov *et al.*, *Nature (London)* **438**, 197 (2005); Y. Zhang *et al.*, *ibid.* **438**, 201 (2005).
- ⁴J. Nilsson *et al.*, *Phys. Rev. B* **78**, 045405 (2008).
- ⁵E. McCann, *Phys. Rev. B* **74**, 161403 (2006).
- ⁶J. B. Oostinga *et al.*, *Nature Mater.* **7**, 151 (2008).
- ⁷Y. Zhang *et al.*, *Nature (London)* **459**, 820 (2009).
- ⁸K. F. Mak *et al.*, *Phys. Rev. Lett.* **102**, 256405 (2009).
- ⁹S. V. Morozov *et al.*, *Phys. Rev. Lett.* **100**, 016602 (2008).
- ¹⁰S. Adam and S. Das Sarma, *Phys. Rev. B* **77**, 115436 (2008).
- ¹¹M. I. Katsnelson, *Phys. Rev. B* **76**, 073411 (2007).
- ¹²M. Koshino and T. Ando, *Phys. Rev. B* **73**, 245403 (2006).
- ¹³J.-H. Chen *et al.*, *Solid State Commun.* **149**, 1080 (2009)
- ¹⁴J.-H. Chen *et al.*, *Nat. Phys.* **4**, 377 (2008).
- ¹⁵E. H. Hwang *et al.*, *Phys. Rev. Lett.* **98**, 186806 (2007).
- ¹⁶C. Jang *et al.*, *Phys. Rev. Lett.* **101**, 146805 (2008).
- ¹⁷S. Adam *et al.*, *Proc. Natl. Acad. Sci. U.S.A.* **104**, 18392 (2007).
- ¹⁸See supplementary material at <http://link.aps.org/supplemental/10.1103/PhysRevB.82.041406> for photomicrograph of the device, Raman spectrum of the device, and RPA results.

¹⁹A. C. Ferrari *et al.*, *Phys. Rev. Lett.* **97**, 187401 (2006).

²⁰M. Ishigami *et al.*, *Nano Lett.* **7**, 1643 (2007).

²¹Note that the Ref. 10 calculates the per-valley per-spin conductivity of BLG, which should be multiplied by four to obtain the total conductivity to compare with the measured values in this work.

²²M. Caragiu and S. Finberg, *J. Phys.: Condens. Matter* **17**, R995 (2005).

²³We have also calculated (Ref. 18) the charged impurity scattering rate in BLG using the RPA screening function for the parabolic dispersion from Ref. 24. Similar results were obtained in Ref. 25. The differences between RPA and TF are of similar magnitude to the uncertainties introduced by the impurity distance d , or the dispersion (parabolic vs hyperbolic) (Ref. 18).

²⁴E. H. Hwang and S. Das Sarma, *Phys. Rev. Lett.* **101**, 156802 (2008).

²⁵S. Das Sarma, E. H. Hwang, and E. Rossi, *Phys. Rev. B* **81**, 161407 (2010).

²⁶T. Ando, *J. Phys. Soc. Jpn.* **75**, 074716 (2006).

²⁷A. N. Pal and A. Ghosh, *Phys. Rev. Lett.* **102**, 126805 (2009).

²⁸S. Das Sarma (private communication).

²⁹Y. Lin and P. Avouris, *Nano Lett.* **8**, 2119 (2008).